16th World Conference on Earthquake, 16WCEE 2017
Santiago Chile, January 9th to 13th 2017
Paper N° 1474 (Abstract ID)
Registration Code: S-M1461322156

VARIATION OF DAMPING REDUCTION FACTORS USED IN DESIGN OF ISOLATED STRUCTURES DUE TO GROUND MOTION DIRECTIONALITY

G. Ozdemir[(1)], B. Bayhan[(2)]

[(1)] *Assoc. Prof., Anadolu University Civil Engineering Department, gokhan_ozdemir@anadolu.edu.tr*
[(2)] *Assoc. Prof., Bursa Technical University Civil Engineering Department, beyhan.bayhan@btu.edu.tr*

Abstract

In seismic isolated structures, the level of equivalent damping ratio is generally greater than 5%. However, the elastic design response spectrum provided by codes specifications are for 5% critical damping. Thus, it has to be modified so that the effect of high damping can be considered. This is achieved by using damping reduction factors. In this study, variation in damping reduction factors due to ground motion orientation has been investigated. Accordingly, orthogonal horizontal components of selected as-recorded ground motions were rotated from 0^o to 180^o with increments of 10^o to mimic various ground motion orientations. Then, damping reduction factors of all the rotated records and the original ones were computed for various damping ratios. Computed values are used to assess the amount of variation in damping reduction factors as a function of ground motion orientation. Results of this study indicate that ground motion orientation is a significant parameter in computation of damping reduction factor.

Keywords: damping reduction factor; ground motion directionality; seismic isolation

1. Introduction

Seismic performance of a structure can be enhanced with application of seismic isolation technique by introducing an isolation level with low flexibility in the horizontal directions. Such a construction technique results in minimized floor accelerations and inter-story drifts together with reduced seismic forces transmitted to the superstructure. But, the expense of such enhancement in the seismic performance of the structure is the amplified isolator displacements that has to be controlled. Therefore, the behavior of a seismic isolated structure is generally dominated by maximum isolator displacement (MID). Although, the most reliable way to predict MIDs is to perform nonlinear response history analyses (NRHA), simplified methods are also established to be used in the design.

In the simplified method of analysis namely, equivalent lateral force (ELF) procedure, the seismic isolators are represented by idealized equivalent linear properties of the isolation units. This method addresses an iterative solution method in which the equivalent damping ratio of the isolator, computed by considering its hysteretic energy dissipation, is employed. Generally, in seismic isolated structures, the level of equivalent damping ratio is greater than 5%, but the elastic response spectrum provided by code specifications are for 5% critical damping. Thus, the iterative method followed in ELF procedure needs a modification in the elastic design spectrum described by code specifications to account for the effects of damping ratios greater than 5%. This can simply be achieved by dividing the 5% design spectrum by a factor called as damping reduction factor, *B*:

$$B = \frac{S_a(T, 5\%)}{S_a(T, \beta)} \tag{1}$$

In Eqn. (1), T is the elastic period of the structure, β is the damping ratio and S_a is the pseudo-spectral acceleration. Computation of *B* by means of Eqn. (1) is actually specific to employed ground motion characteristics. It may vary for each ground motion record. Thus, the dependency of *B* to ground motion characteristics has been studied by several researchers [1-10]. Parameters considered in these studies were soil characteristic, type of fault rupture, number of cycles, duration and magnitude of ground motion. There are also studies used as a basis for code specifications [10]. Nevertheless, none of the aforementioned studies focused on variation of *B* as a function of ground motion orientation. In previous studies, either the original as-recorded ground motions or their components in both fault-parallel and fault-normal directions are used in computations. However, the ground motion characteristics [11,12], thereby the dynamic response of structures [13-16] depends highly on the orientation of the sensors used in recording the ground motion.

The objective of this study is to determine the sensitivity of damping reduction factor, *B*, to variation in ground motion orientation. For this purpose, a group of as-recorded ground motions are rotated through 180^o with 10^o intervals and the corresponding *B* values are computed. Once the computations are established for several damping ratios, *B* values provided by codes are also compared with the computed ones.

2. As-Recorded Ground Motion Set

In this study, 10 near-field ground motion records are used to investigate the variation in *B* due to change in ground motion orientation. Selected records have moment magnitudes (M_w) ranging from 6.5 to 7.5 and closest distances to fault rupture (R) less than 20 km. All ground motion records are downloaded from PEER Strong Ground Motion Database [17]. The soil group of these records is class D per NEHRP [18] where the average shear wave velocities at the upper most 30 m soil profile are ranging from 180 m/s to 360 m/s. Selection of ground motions is also achieved by considering the research outputs of Avsar and Ozdemir [19]. According to research outputs of Avsar and Ozdemir [19], peak ground velocity (PGV) has the best correlation with MIDs among the commonly used ground motion intensity measures. Authors also stated that correlation of PGV with MIDs is not sensitive to any change in isolator characteristics. Since the response quantity estimated by the ELF procedure is MID and *B* is an input to this procedure, it is believed that it would be appropriate to use PGV as a criteria in ground motion selection. As a result, in addition to M_w, R and soil class, PGV is also considered in selection of as-recorded ground motions. Table 1 presents the characteristics of selected ground motions. PGV values of ground motions presented in Table 1 varies in between 30cm/s and 50cm/s. The corresponding 5% damped response spectra are presented in Fig. 1. While constructing the 5% damped response spectra of the horizontal components of a ground motion, the spectra that correspond to "strong" and "weak" components are identified accordingly. Here, the term "strong" is used to identify the horizontal component with higher PGV compared to other orthogonal horizontal component of the same record. In Table 1, PGA stands for peak ground acceleration and PGD represents peak ground displacement.

Table 1 – Characteristics of ground motion records used in computations

#	Earthquake	Station	M_w	R (km)	Component	PGA (g)	PGV (cm/s)	PGD (cm)
1	Imperial Valley	Brawley Airport	6.5	10.4	315	0.22	38.9	13.6
					225	0.16	35.8	22.3
2	Imperial Valley	Bonds Corner	6.5	2.6	230	0.77	45.9	15.0
					140	0.59	45.2	16.7
3	Imperial Valley	El Centro Array #10	6.5	6.2	050	0.17	47.5	31.1
					320	0.22	41.2	18.0
4	Loma Prieta	Gilroy Array #2	6.9	11.1	090	0.32	39.1	12.2
					000	0.37	32.9	7.0
5	Loma Prieta	Gilroy Array #3	6.9	12.8	090	0.37	44.7	19.4
					000	0.56	35.7	8.4
6	Northridge	Canyon Country W Lost Canyon	6.7	12.4	270	0.48	44.9	12.6
					000	0.41	43.0	11.8
7	Superstition Hills	El Centro Imp Co Center	6.5	18.2	000	0.36	46.4	17.4
					090	0.26	40.9	20.0
8	Chi-Chi	TCU138	7.6	9.8	E	0.19	41.0	36.4
					N	0.22	40.9	26.1
9	Chi-Chi	CHY035	7.6	12.7	W	0.25	45.6	12.0
					N	0.25	37.7	16.9
10	Chi-Chi	TCU050	7.6	9.5	N	0.13	42.4	52.0
					W	0.15	36.9	54.7

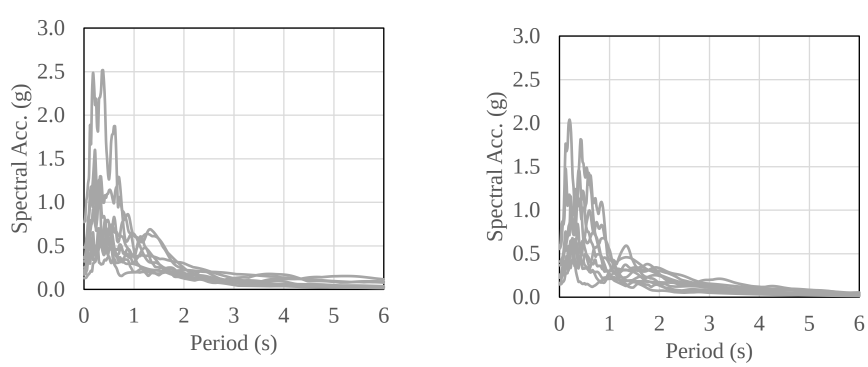

(a) for strong components (b) for weak components

Fig. 1 – 5% damped elastic response spectra of the selected as-recorded ground motions.

3. Rotation of Selected Ground Motions

In order to obtain different orientations of ground motion records, orthogonal horizontal components of the selected records are rotated through 180^o with 10^o intervals. Rotating the ground motion components through 180^o, the orthogonal horizontal components of any ground motion will replace each other. Thus, considering only one of the two orthogonal horizontal components will be sufficient in computing the *B* values through several angles. Rotation of horizontal components is performed in accordance with Eqn. (2) where $a_x(t)$ and $a_y(t)$ are the accelerations of orthogonal horizontal components of the as-recorded motion, and $a(\theta,t)$ represents the acceleration for one of the rotated components.

$$a(\theta, t) = a_x(t)\cos\theta + a_y(t)\sin\theta \tag{2}$$

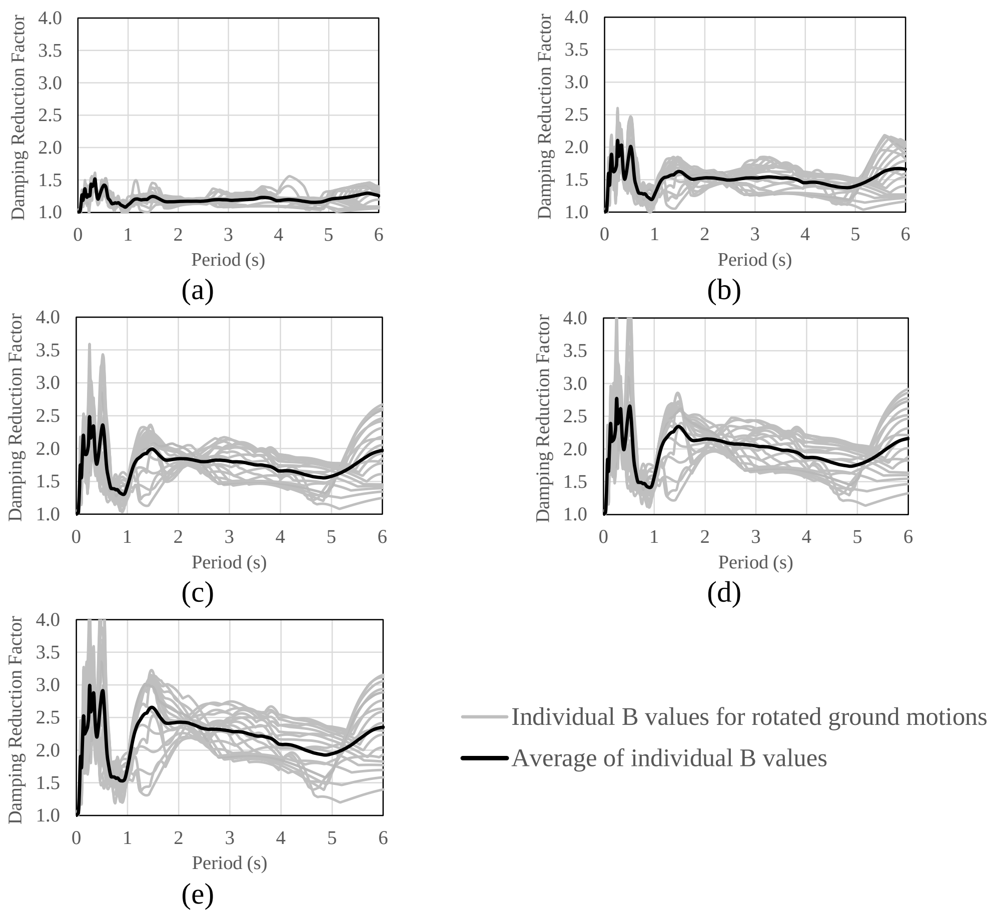

Fig. 2 – Variation of *B* due to rotation of El Centro Array #10 record of Imperial Valley for damping ratios of (a)10% (b)20% (c)30% (d)40% (e)50%.

4. Research Methodology

Once the orthogonal horizontal components of an as-recorded ground motion are rotated through several angles, the next step is to compute the corresponding *B* values. In computations, elastic response spectra of the rotated ground motion record are constructed for different levels of damping ratios namely, 5%, 10%, 20%, 30%, 40% and 50%. Then, corresponding *B* values are computed by means of Eqn. (1). Since using one horizontal component is enough in computations, the "strong" component is considered only. To clarify the variation in *B* as a function of ground motion orientation, El Centro Array #10 record of Imperial Valley is studied in detail.

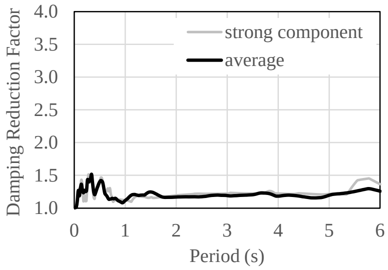

(a) 10% damping

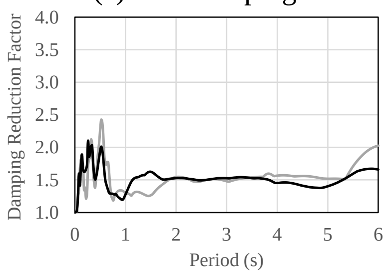

(b) 20% damping

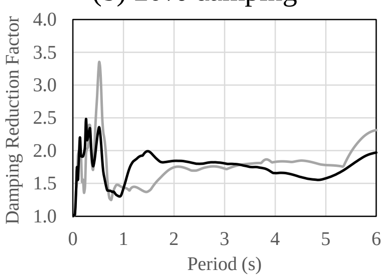

(c) 30% damping

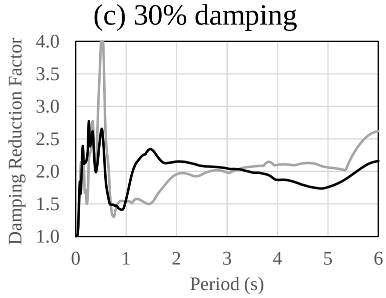

(d) 40% damping

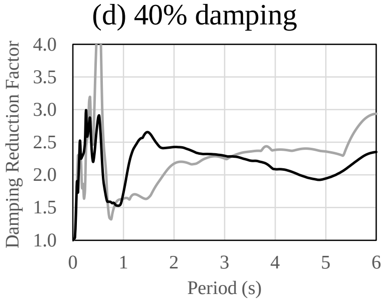

(e) 50% damping

Fig. 3 – Comparison of average $B_{rotated}$ with the ones computed by “strong” component of original record for Imp.Val.El Centro Array #10.

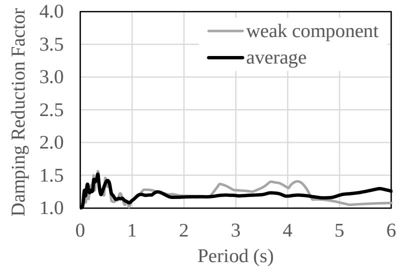

(a) 10% damping

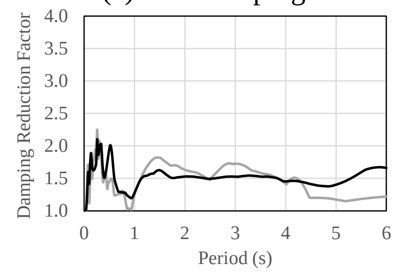

(b) 20% damping

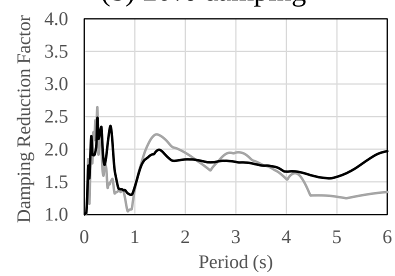

(c) 30% damping

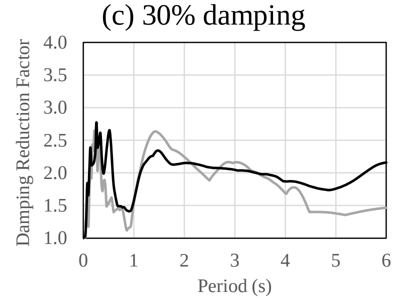

(d) 40% damping

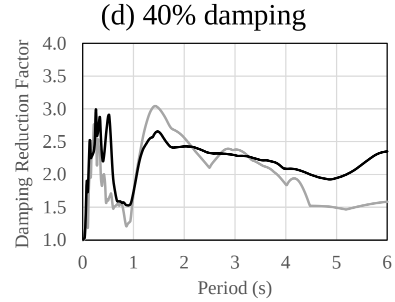

(e) 50% damping

Fig. 4 – Comparison of average $B_{rotated}$ with the ones computed by “weak” component of original record for Imp.Val.El Centro Array #10.

Fig. 2 presents the variation in damping reduction factors due to rotation of El Centro Array #10 record of Imperial Valley for different levels of damping ratios. In Fig. 2, each grey line represents the computed *B* values for different orientations of El Centro Array #10. On the other hand, black lines stand for the average of these individual *B* values. Fig. 2 clearly demonstrates that the damping reduction factor varies due to the orientation of the ground motion. And, the amount of variation is dependent of the period. However, there is not any consistent relation between period and variation in *B* when different ground motion orientations are of concern. To identify the differentiation in *B* values of both the original as-recorded motions and the rotated forms, Fig. 3 and 4 are depicted. In these figures, averages of *B* values represented by black solid lines in Fig. 2 are compared with the ones computed for the "strong" and "weak" components of the as-recorded ground motion. It is clear that *B* values computed by employing the orthogonal horizontal components of as-recorded ground motion differ from the average of *B* values determined for various orientations. This differentiation is observed to be a function of the level of damping ratio. Based on Figs. 2-4, it can be said that the sensitivity of *B* to ground motion orientation increases with increasing damping ratio. Figs. 2-4 also reveal that using the "strong" component of a ground motion to compute *B* may result in higher values at periods larger than 3s. (a typical value for effective period of seismic isolated structures) compared to average *B* values computed by considering the rotated forms of records. Thus, the ELF procedure may give unsafe results in terms of MID.

5. Code Specifications for *B*

In this section, comparison of *B* values suggested by codes provisions (see Table 2) with those computed by means of Eqn. (1) for all of the ground motions orientations is discussed. For this purpose, *B* values of each ground motion record rotated by 10^{o} intervals are computed and their average is considered (see Fig. 2). Once, average *B* values for all individual ground motion records have been established, further averaging these values will provide the *B* values as a function of ground motion directionality in an average sense. Employing the average values to represent the variation in *B* is based on the decision of using arithmetic mean values of a normal probability distribution for the response spectral ordinates [20]. Comparisons are depicted in Fig. 5 for damping ratios up to 50%.

Table 2 – Code suggested values for *B*.

β %	ASCE/AASHTO	NEHRP	EUROCODE 8
≤ 2	0.8	0.8	0.8
5	1.0	1.0	1.0
10	1.2	1.2	1.2
20	1.5	1.5	1.6
30	1.7	1.8	1.9
40	1.9	2.1	2.1
50	2.0	2.4	2.3

In Fig. 5, dashed lines represent the recommended *B* values of the code provisions whereas the solid lines stand for the computed *B* values (average (average (B_{rotated})), here B_{rotated} is the *B* value calculated for the rotated ground motion record). Based on Fig. 5, *B* values suggested by code provisions (dashed lines) will be deemed as conservative when they are less than the computed ones (solid lines). Fig. 5a presents the comparison of *B* values suggested by ASCE/AASHTO [21,22] with the computed ones for different damping ratios. Fig. 5a revealed that *B* values suggested by ASCE/AASHTO [21,22] are mostly over-conservative especially for damping ratios greater than 20% regardless of the period of the structure. Comparison of *B* values suggested by NEHRP [19] with the ones computed by Eqn. (1) is given in Fig. 5b. As shown in Fig. 5b, NEHRP [18] provides close estimations for the computed *B* values for damping ratios up to 30% when period is greater than 3s. For damping ratios greater than 30%, code suggested values tend to be unconservative. Finally, comparison of computed *B* values with the suggestions of Eurocode 8 [23] is given in Fig. 5c. It is revealed that *B* values recommended by Eurocode 8 [23] are unconservative even at small damping ratios for periods greater than 3s.

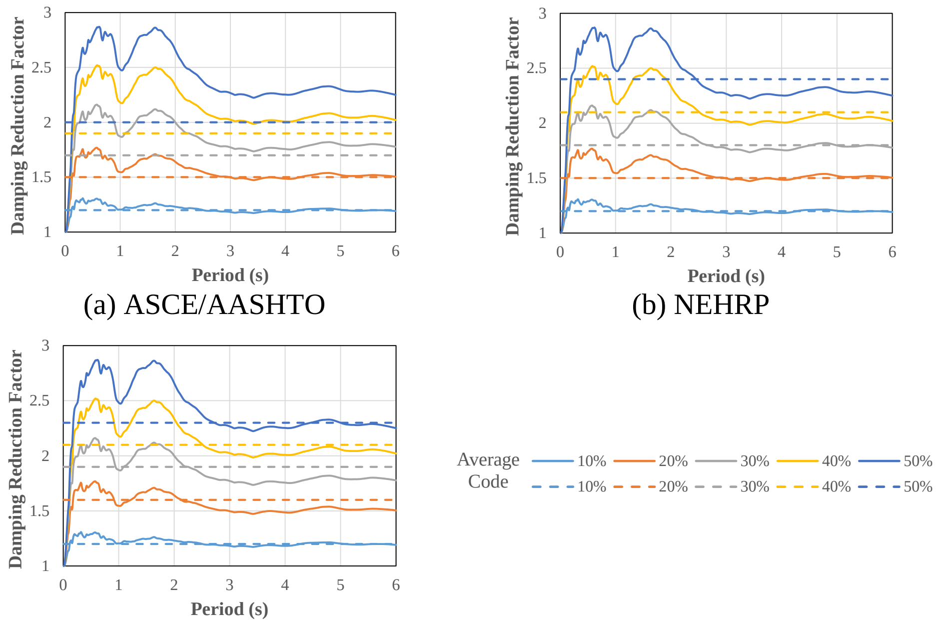

(a) ASCE/AASHTO (b) NEHRP

(c) EUROCODE 8

Fig. 5 – Comparison of average $B_{rotated}$ with code suggested values.

6. Conclusions

In this study, variation in damping reduction factor due to ground motion orientation was studied. For this purpose, a set of ground motions consisting of 10 records were selected and employed in the computations. The as-recorded original forms of the selected ground motions were rotated through 180^o with increments of 10^o to represent different orientations. Suggestions of the existing codes for damping reduction factors were compared with those computed for different orientations. Results of this study revealed the followings:

- *B* is found to be sensitive to ground motion orientation. The amount of differentiation between *B* computed based on original as-recorded form of a ground motion and those computed based on rotated forms was found to be a function of damping ratio. As the damping ratio increases the amount of differentiation also increases.
- NEHRP suggestions for *B* values provide the closest estimations among the assessed code provisions to obtain average *B* values computed by considering the rotated forms of the records. This is especially valid for periods greater than 3s.

7. Acknowledgements

This study is supported by Anadolu University Scientific Research Projects Commission under the grant no: 1505F233.

8. References

[1] Hubbard DT, Mavroeidis GP (2011): Damping coefficients for near-fault ground motion response spectra. *Soil Dynamics and Earthquake Engineering*, 31(), 401-417.

[2] Hatzigeorgiou GD (2010): Damping modification factors for SDOF systems subjected to near-fault, far-fault and artificial earthquakes. *Earthquake Engineering and Structural Dynamics*, 39(),1239-1258.

[3] Cardone D, Dolce M, Rivelli M (2009): Evaluation of reduction factors for high-damping design response spectra. *Bulletin of Earthquake Engineering*, 7(), 273-291.

[4] Stafford PJ, Mendis R, Bommer JJ (2008): Dependence of damping correction factors for response spectra on duration and numbers of cycles. *Journal of Structural Engineering*, 134(), 1364-1373.

[5] Cameron WI, Green RA (2007): Damping correction factors for horizontal ground-motion response spectra. *Bulletin of the Seismological Society of America*, 97(), 934-960.

[6] Lin YY, Miranda E, Chang KC (2005): Evaluation of damping reduction factors for estimating elastic response of structures with high damping. *Earthquake Engineering and Structural Dynamics*, 34(), 427-443.

[7] Lin YY, Chang KC (2004): Effects of site classes on damping reduction factors. *Journal of Structural Engineering*, 130(), 1667-1675.

[8] Lin YY, Tsai MH, Chang KC (2003): On the discussion of the damping reduction factors in the constant acceleration region for ATC-40 and FEMA 273. *Earthquake Spectra*, 19(), 1001-1006.

[9] Ramirez OM, Constantinou MC, Whittaker AS, Kircher CA, Chrysostomou CZ (2002): Elastic and inelastic seismic response of buildings with damping systems. *Earthquake Spectra*, 18(), 531-547.

[10] Naeim F, Kircher CA (2001): On damping adjustment factors for earthquake response spectra. The Structural Design of Tall Buildings, 10(), 361-369.

[11] Rupakhety R, Sigbjörnsson R (2013): Rotation-invariant measures of earthquake response spectra. *Bulletin of Earthquake Engineering*, 11(), 1885-1893.

[12] Boore DM (2010): Orientation-independent, nongeometric-mean measures of seismic intensity from two horizontal components of motion. *Bulletin of the Seismological Society of America*, 100(), 1830-1835.

[13] Kostinakis KG, Athanatopoulou AM, Avramidis IE (2013): Evaluation of inelastic response of 3D single-story R/C frames under bi-directional excitation using different orientation schemes. Bulletin of Earthquake Engineering, 11(), 637-661.

[14] Moschonas IF, Kappos AJ (2013): Assessment of concrete bridges subjected to ground motion with an arbitrary angle of incidence: static and dynamic approach. *Bulletin of Earthquake Engineering*, 11(), 581-605.

[15] Rigato AB, Medina RA (2007): Influence of angle of incidence on seismic demands for inelastic single-storey structures subjected to bi-directional ground motions. *Engineering Structures*, 29(), 2593-2601.

[16] Lopez OA, Torres R (1197): The critical angle of seismic incidence and the maximum structural response. *Earthquake Engineering and Structural Dynamics*, 26(), 881-894.

[17] PEER, Pacific Earthquake Engineering Research Center (2016): Strong Motion Data Base. Available from ngawest2.berkeley.edu.

[18] NEHRP, National Earthquake Hazard Reduction Program (2006): Recommended Provisions for the Development of Seismic Regulations for New Buildings. *Building Seismic Safety Council*, Washington, USA.

[19] [33Avsar O, Ozdemir G (2013): Response of seismic isolated bridges in relation to intensity measures of ordinary and pulse-like ground motions. *Journal of Bridge Engineering*, 18(), 250-260.

[20] Pavlou EA, Constantinou MC (2004): Response of elastic and inelastic structures with damping systems to near-field and soft-soil ground motions. Engineering Structures, 26(9), 1217-1230.

[21] ASCE, American Society of Civil Engineers (2010): Minimum Design Loads for Buildings and Other Structures, *Standard ASCE/SEI 7-10*, Reston, USA.

[22] AASHTO, American Association of State Highway and Transportation Efficials (1999): *Guide Specification for Seismic Isolation Design*, Washington, USA.

[23] EUROCODE 8 (2005): *Design of Structures for Earthquake Resistance Part 2: Bridges*.